Wet-season spatial variability of N_2O emissions from a tea field in subtropical central China

Xiaoqing Fu, Xinliang Liu, Yong Li *, Jianlin Shen, Yi Wang, Ganghua Zou, Hang Li, Lifang Song, Jinshui Wu

Changsha Research Station for Agricultural & Environmental Monitoring and
Key Laboratory of Agro-ecological Processes in Subtropical Regions,
Institute of Subtropical Agriculture, Chinese Academy of Sciences,
Hunan 410125, China

These two authors contributed equally to this work.

*Correspondence to: Professor Yong Li
Institute of Subtropical Agriculture,
Chinese Academy of Sciences, Hunan 410125, China
Tel: +86-731-8461-5291
Fax: +86-731-8461-2685
E-mail: yli@isa.ac.cn

Abstract

Tea fields emit large amounts of nitrous oxide (N_2O) to the atmosphere. Obtaining accurate estimations of N_2O emissions from tea-planted soils is challenging due to strong spatial variability. We examined the spatial variability of N_2O emissions from a red-soil tea field in Hunan province, China, on 22 April 2012 (in a wet season) using 147 static mini chambers approximately regular gridded in a 4.0 ha tea field. The N_2O fluxes for a 30-min snapshot (10:00-10:30 am) ranged from -1.73 to 1,659.11 g N ha^{-1} d^{-1} and were positively skewed with an average flux of 102.24 g N $ha^{-1}d^{-1}$. The N_2O flux data were transformed to a normal distribution by using a logit function. The geostatistical analyses of our data indicated that the logit-transformed N_2O fluxes (FLUX30t) exhibited strong spatial autocorrelation, which was characterized by an exponential semivariogram model with an effective range of 25.2 m. As observed in the wet season, the logit-transformed soil ammonium-N (NH4Nt), soil nitrate-N (NO3Nt), soil organic carbon (SOCt), total soil nitrogen (TSNt) were all found to be significantly correlated with FLUX30t (r=0.57-0.71, p< 0.001). Three spatial interpolation methods (ordinary kriging, regression kriging and cokriging) were applied to estimate the spatial distribution of N_2O emissions over the study area. Cokriging with NH4Nt and NO3Nt as covariables (r=0.74 and RMSE=1.18) outperformed ordinary kriging (r=0.18 and RMSE=1.74), regression kriging with the sample position as a predictor (r=0.49 and RMSE=1.55) and cokriging with SOCt as a covariable (r=0.58 and RMSE=1.44). The predictions of the three kriging interpolation methods for the total N_2O emissions of 4.0 ha tea field ranged from 148.2 to 208.1 g N d^{-1}, based on the 30 min snapshots obtained during

the wet season. Our findings suggested that to accurately estimate the total N_2O emissions over a region, the environmental variables (e.g., soil properties) and the current land use pattern (e.g., tea row transects in the present study) must be included in spatial interpolation. Additionally, compared with other kriging approaches, the cokriging prediction approach showed great advantages in being easily deployed, and more importantly providing accurate regional estimation of N_2O emissions from tea-planted soils.

Introduction

According to the latest data, which show rapid increases in their atmospheric concentrations (IPCC, 2013), nitrous oxide (N_2O), carbon dioxide (CO_2) and methane (CH_4) are three major greenhouse gases in the atmosphere that significantly contribute to global warming. Among these major greenhouse gases, N_2O has a very high radiative forcing per unit mass (265-fold stronger than CO_2 on a 100 year horizon) and plays an important role in ozone depletion in the stratosphere (Ravishankara et al., 2009). The primary sources of N_2O are from agriculture development and the subsequent increased use of chemical N fertilizers (Ambus and Christensen, 1994; Mosier et al., 1996, 1998; Yanai et al., 2003; Tokuda and Hayatsu, 2004; Akiyama et al., 2006; Ravishankara et al., 2009). Agricultural soils produce 2.8 (1.7–4.8) Tg of N_2O-N yr^{-1} (IPCC, 2013). The N_2O is emitted from soils via the microbial processes of nitrification under aerobic conditions and denitrification under anaerobic conditions (Firestone and Davidson, 1989; Wrage et al., 2004). The magnitude of soil N_2O emissions is highly variable and strongly influenced by changes in environmental conditions.

Among the different agricultural soils, tea-planted soils are important sources of N_2O that are rapidly attracting attention due to recent large increases in the number of tea plantations and large N fertilizer inputs (Akiyama et al., 2006; Lin and Han, 2009; Fu et al., 2010, 2012; Hirono and Nonaka, 2012; Han et al., 2013; Li et al., 2013). In China, the total tea-planted area was approximately 2.10 million ha (mostly distributed in Fujian, Anhui, Zhejiang and Hunan) in 2013 (NBSC, 2014). Compared with other agricultural soils, tea-planted soils provide optimal conditions (e.g., low soil pH, high temperature and ample moisture) for microbes to emit significant amounts of N_2O (Hayatsu, 1993; Venterea and Rolston, 2000; Li et al., 2013). However, because few measurements of N_2O emissions from tea-planted soils have been reported in China (Fu et al., 2012; Li et al., 2013; Han et al., 2013), it is difficult to conduct precise spatial and temporal evaluations of N_2O emissions from tea-planted soils. To estimate the N_2O emissions from tea-planted soils accurately and to understand the roles that tea plantations play in global warming, it is necessary to investigate the spatial and temporal patterns and related mechanisms of N_2O emissions from tea fields. This information will lead to the development of effective land management options for mitigating N_2O emissions from a significant source, tea plantation.

The N_2O fluxes have large spatial variability in agricultural soils (Konda et al., 2008, 2010; Meda et al., 2012; Li et al., 2013). Many previous studies in tea fields have found pronounced seasonal fluctuations in N_2O fluxes, with higher N_2O emissions during the wet season than during the dry season (Fu et al., 2012; Han et al., 2013). The seasonal and spatial variability of N_2O emissions significantly contributes to the uncertainty when estimating the

81 contributions of subtropical tea-planted ecosystems to N_2O flux. Moreover, most of our
82 knowledge regarding seasonal changes and the spatial variability of N_2O fluxes is based on a
83 small number of measurements taken from tea-planted soils. Li et al. (2013) investigated the
84 spatial structure of N_2O fluxes for tea-planted soils during the dry season in October 2010
85 and found that the spatial distribution of the N_2O fluxes was primarily associated with field
86 elevation (r=-0.42, p<0.001). The other soil properties (e.g., soil organic carbon, soil water
87 and soil mineral nitrogen) were not significantly related to N_2O flux. To obtain a more
88 accurate evaluation of the interannual variability of N_2O emissions from tea-planted soils, a
89 study on the spatial structure and distribution of N_2O emissions during a wet season (in
90 contrast to the dry season) is necessary.
91 To understand the structure of the spatially distributed data and to predict the N_2O fluxes
92 at the unsampled locations, geostatistical analyses can be useful (Goovaerts, 1997; Webster
93 and Oliver, 2001). Geostatistics provide statistical tools for describing the quantitative spatial
94 variability of field observations for the accurate mapping and planning of rational sampling
95 schemes that efficiently utilize the available labor (Webster, 1985). Several geostatistical
96 methods are used to examine the spatial variability of N_2O fluxes, including simple kriging
97 (SK), ordinary kriging (OK), regression kriging (RK) and cokriging (CK). The most
98 commonly used method is OK (Clemens et al., 1999; Röver et al., 1999; Mathieu et al., 2006;
99 Konda et al., 2008, 2010), which uses the derived theoretical semivariogram models to
100 interpolate the spatial distribution of N_2O fluxes. However, research has demonstrated that
101 RK and CK approaches, which use related auxiliary variables, improve the prediction

accuracy (Goovaerts, 1997; Webster and Oliver, 2001; Hengl et al., 2004). The RK method combines multiple regressions, including linear regressions, generalized linear models, generalized added models and regression tree models, with the auxiliary variables used for kriging (Odeh et al., 1994). In the RK method, linear regressions are commonly used. The CK approach uses correlations that may exist between the predicted variables and other more easily measured variables. These variables can be measured at the same points as the predicted variable, at other points, or at both. Compared with the RK approach, the CK approach is commonly applied when the measurement of a covariable is less expensive than the cost of a predicted variable (Stein et al., 1988; Odeh et al., 1995). In addition to the feature correlation as a criterion for selecting covariables, the CK approach also requires that both of the predicted variable and covariables have similar spatial structures (Odeh et al., 1994). In this study, we used three interpolation methods (OK, RK and CK) to estimate the spatial distribution of N_2O fluxes in a tea field.

In contrast with the dry season, the spatial variability of the N_2O emissions was investigated during the wet season in April 2012 from the same tea-planted catchment that was studied by Li et al. (2013). The catchment consisted of a completely independent hydrological system. Thus, the spatial distribution of the N_2O emissions within the catchment was expected to have intrinsic characteristics. The objectives of this study were to (i) evaluate the spatial variability of N_2O emissions from soils planted with tea in subtropical central China during the wet season, (ii) determine the key environmental factors controlling N_2O emissions, and (iii) assess the prediction efficiency of three kriging interpolation methods.

2. Materials and Methods

2.1 *Site description*

The field experiment was conducted in a small catchment (4.0 ha) in Jinjing, Changsha, in Hunan province, China (28˚32′50″N and 113˚19′58″ E and elevation 90 to 111 m) (Fig. 1). The region has a subtropical monsoon climate with a mean annual air temperature of 17.5°C and a mean annual precipitation of 1400 mm (average from 1979 to 2012). The site had four distinct seasons: spring (February to April), summer (May to July), autumn (August to November), and winter (December to January). On average, 70% of the annual precipitation occurred in April, May and June. The daily air temperature and precipitation for 2012 were recorded by an automatic weather station (Intelimet A, IMET-ADV2, Dynamax, USA) located next to the studied catchment (Fig. 2). The soil of the catchment was a Haplic Alisol (FAO/UNESCO soil taxonomy) that was derived from a granitic parental material. Tea (*Camellia sinensis L., cv. Baihaozao*) was contour-planted 10 years ago using an inter-row spacing of 0.5 m in the catchment.

<Insert Fig. 1 & Fig. 2 near here>

2.2 *Sampling positions*

In the 4.0 ha tea-planted catchment, 1964 evenly-distributed points with plane coordinates and elevation values and 456 centerlines of tea tree row were recorded by locally calibrated differential Geographic Positioning System (DGPS) receiver (Sanding Southern Survey Co.,

China), and then were used to develop the local DEM and land use data (at a spatial resolution of 0.1 m, respectively, as shown in Fig. 1c and d). The land use data showed the four positions where the chambers were placed, including the inter-row, fertilization point, under tea tree and in tea tree row, as described in Li. et al. (2013). The spatial positions of the gas sampling points in a 15 m × 15 m regular grid over the catchment were originally determined using a DGPS receiver on 20 April 2012. Some of the chamber positions were slightly adjusted (because of a lack of space in the tea tree rows or to avoid roads and trenches). Thus, the chambers were placed in one of four locations mentioned above (Fig. 1d). Overall, 147 sampling points were determined, and the Euclidean distances between each point and its nearest neighbors ranged from 14.6 m to 16.7 m. The x-y coordinates, the gas sampling position information (the inter-row, fertilization point, under tea tree and in tea tree row along tea row transects), and the elevations at the sampling points were recorded.

2.3 *Gas and soil properties measurements*

Gas and soil samples were collected at each grid point on 22 April 2012 using a closed mini chamber technique. A mini chamber set was composed of PVC and had two parts (base and chamber). The base was 0.15 m in diameter and 0.05 m high. The chamber was 0.15 m in diameter and 0.15 m high, and was equipped with rubber septa on the top for gas sampling. In the field operation, the base was gently inserted vertically into the soil on 20 April 2012, and the chamber was clipped on the base with the sponge seals in between to stop gas leaking before gas sampling on 22 April 2012. Therefore, the effective static chambers volume was

166 equal to the chamber volume of 0.002651 m^3. Gas samples were collected from the
167 headspace between 10:00 and 10:30 am. For simultaneous sampling, 25 skilled gas sampling
168 persons helped to accomplish the field sampling. Each person only took care of one column
169 containing 4 to 8 sampling positions (see Fig. 1), and started sampling at the same time of 10
170 am. At each point, three gas sample replicates were collected from the headspace into
171 pre-evacuated 12 mL vials (Exetainers, Labco, UK) at 0 and 30 min after the chamber body
172 was clipped. After collecting the gas samples, the air temperature in each chamber was
173 measured for subsequent correction of the flux calculation, and then three replicate soil cores,
174 0.05 m in diameter and 0.20 m in depth, were collected from the soils inside the mini
175 chambers. Soil samples were put straight into clean zip-lock bags for avoiding soil moisture
176 loss, and quickly transported back to the laboratory in thermal insulation boxes and stored in
177 a refrigeration room at 4 ^oC for preventing any microbial activity (such as mineralization,
178 nitrification and denitrification). The N_2O concentrations of the gas samples were analyzed
179 using a gas chromatograph (Agilent 7890A, Agilent, USA) that was fit with a ^{63}Ni-electron
180 capture detector and an automatic sample injector system. The N_2O fluxes (FLUX30, g N ha^{-1}
181 d^{-1}) were calculated as described by Li et al. (2013). The soil physical/chemical properties
182 determined by using fresh soil, e.g., the soil ammonium content (NH4N), soil nitrate content
183 (NO3N), soil dissolved organic carbon content (DOC), soil volumetric water content (SWC),
184 and soil bulk density (BD), were measured within three days after sampling, while those
185 using air-dried soil, e.g., total soil nitrogen content (TSN), soil organic carbon content (SOC)
186 and soil clay/silt/sand content (CLAY, SILT and SAND), were determined within two weeks

187 after the field work.

188

189 2.4 *Data analyses*

190 The descriptive statistical and geostatistical analyses were performed using R (R
191 Development Core Team, 2014) with the gstat package (DGUU, 2010).

192 Descriptive statistical analyses were used to determine the mean, median, minimum and
193 maximum values, SD, coefficient of variation (CV), and skewness of the original and
194 logit-transformed data. These analyses were based on the four chamber placement positions.
195 Because the FLUX30, NH4N, NO3N, SOC, TSN and SWC data were highly skewed, these
196 values were transformed by using a logit function (Hengl et al., 2004). The transformed
197 variables were named FLUX30t, NH4Nt, NO3Nt, SOCt, TSNt and SWCt. Using a Pearson's
198 correlation, the relationships between FLUX30t, NH4Nt, NO3Nt, SOCt, TSNt, SWCt, DOC,
199 BD, SAND, SILT, and CLAY were tested. The significance of the differences in the FLUX30t
200 and environmental factors (NH4Nt, NO3Nt, SOCt, TSNt and DOC) between any two of the
201 different chamber positions along the entire tea-tree row transect were evaluated using the
202 Tukey's Honest Significant Difference method.

203 In the geostatistical analyses, an experimental semivariogram of FLUX30t was
204 calculated, and the theoretical semivariogram models were fit. The ratio of the partial sill to
205 the total sill was used as an index of spatial dependence. Armstrong (1998) stated that a
206 variable with a higher ratio of partial sill to sill and a longer semivariogram range were more
207 structured. The spatial distribution of FLUX30t across the catchment was predicted using

three kriging interpolation methods (OK, RK and CK).These data were transformed back to the original scale of FLUX30 for mapping. The Leave-One-Out cross-validation method was used to evaluate the accuracy of interpolating FLUX30t using the three different kriging methods.

3. Results

3.1 *Exploratory data analyses*

In the 4.0 ha tea-planted catchment, the N_2O fluxes during the 30-min one-time measurements performed on 22 April 2012 ranged from -1.73 to 1,659.11 g N ha^{-1} d^{-1}, with a median value of 27.56 g N ha^{-1} d^{-1} and a CV of 234.7 % (Table 1). The N_2O flux data were positively skewed (Table 1 and Fig. 3a), and their logit-transformations were approximately normally distributed (Table 1 and Fig. 3b). From Table 3, the logit-transformed N_2O fluxes (FLUX30t) were the highest in the fertilization points, and the differences in the FLUX30t values among the chamber placement positions were statistically significant ($p < 0.001$).

<Insert Table 1 & Fig. 3 near here>

The ELEVATION, BD, DOC, SWC, SAND, SILT, and CLAY were approximately normally distributed, with skewness values of less than 1 (Table 1). Additionally, DOC displayed a moderate CV of 34.6 %, and the other variables had lower CVs (4.1–23.8 %). The NH4N, NO3N, SOC and TSN were positively skewed, and the logit-transformations (NH4Nt,

NO3Nt, SOCt and TSNt) had approximately normal distributions (Table1). The NH4N and NO3N had very high CVs (190.8 % and 141.6 %, respectively), and the SOC and TSN had moderate CVs (50.1 % and 38.3 %, respectively).

The NH4Nt, NO3Nt, SOCt, TSNt and SWC were significantly correlated with the N_2O fluxes (Fig. 5), and the NH4Nt, NO3Nt and TSNt had strong positive relationships with N_2O ($r = 0.71$, 0.70 and 0.57, respectively, $p < 0.001$). The N_2O emissions and some soil properties (NH4N, NO3N, SOC, TSN and SWC) in the fertilization points were significantly different ($p < 0.001$) from the other three chamber placement positions (Fig. 6). These variables were used as auxiliary covariables for the CK approach.

<Insert Fig. 4 & Fig. 5 near here>

3.2 *Spatial variability of N_2O emissions and related environmental factors*

Because most of the soil properties were significantly correlated with the chamber placement positions, two types of semivariogram models were calculated for the N_2O and soil parameters (correlated with N_2O fluxes) in the wet season (Table 2). The FLUX30t exhibited strong spatial autocorrelation and was characterized by an exponential semivariogram model, a theoretical distance parameter of 8.40 m (equivalent to an effective range of 25.2 m) and a zero nugget. The NH4Nt, SWCt, SAND and SILT showed almost no spatial dependency, while NO3Nt and TSNt demonstrated weak spatial dependency with a range parameter of 91.9 and 58.0 m, respectively (equivalent to an effective range of 163.7 and 102.6 m,

250 respectively).The SOCt exhibited a moderate spatial dependency within 93.0 m. By
251 detrending the influence of the chamber placement position, large changes in the
252 semivariogram models occurred regarding the above variables. Although the semivariograms
253 of the regression residuals of FLUX30t, NH4Nt, NO3Nt and SOCt were best-fit with the
254 same semivariogram model (exponential) with a similar range of 17.4 m (equivalent to an
255 effective range of 52.1 m), the spatial dependencies of those variables were different (Table
256 2). Of the soil properties, only SOCt had a similar spatial structure to FLUX30t when the
257 influence of the chamber placement position was detrended (Table 2). Based on these
258 correlation analyses and spatial variability analyses, the covariables for the CK method were
259 determined.
260
261 *<Insert Table 2 near here>*
262
263 3.3 *Spatial interpolation of N_2O emissions by three methods*
264 Three spatial interpolation methods were used in this study to predict the spatial distribution
265 of N_2O emissions from tea soils in the catchment. In the first method, the derived theoretical
266 semivariogram model for FLUX30t that is presented in Table 2 was used for the OK
267 prediction. In the second method, RK was used and the chamber placement position was
268 identified as the auxiliary regression predictor. Thus, the semivariogram of the regression
269 residuals of FLUX30t were calculated and best-fit with the theoretical semivariogram model
270 shown in Fig. 6. In the third method, CK involved two groups of covariables. As described

271 previously, because SOCt (detrending the influence of chamber placement position) showed a
272 similar spatial structure to FLUX30t (detrending the influence of chamber placing position), a
273 CK process was performed using SOCt as the covariable. Firstly, the direct and
274 cross-semivariograms of FLUX30t and SOCt (detrending the influence of the chamber
275 placement position) were calculated and best-fit with a linear model for co-regionalization
276 (LMC). Next, the fitted LMC was used to predict the spatial surface of N_2O emissions.
277 Because NH4Nt and NO3Nt were significantly correlated with FLUX30t (Fig. 5), a second
278 CK with NH4Nt and NO3Nt as the covariables was processed, similarly to that of the CK
279 with SOCt. However, these covariables had different spatial structures (Table 2). As reflected
280 by the lower root mean squared error (RMSE) and higher *r* values (Table 4), the CK method
281 performed better than the other spatial interpolation methods. Furthermore, the CK with
282 NH4Nt and NO3Nt as two covariables outperformed the CK with SOCt as the covariable.
283
284 *<Insert Figs.6-9 near here>*
285
286 As shown in Fig. 9, the surface map for the spatial distribution of N_2O emissions
287 interpolated by OK was rougher than the maps obtained from the other interpolation
288 approaches. The kriging standard deviation maps were showed in Fig. 10, and clearly
289 indicated that the RK and CK methods with lower kriging standard deviations outperformed
290 the OK method with higher kriging standard deviations. The four kriging interpolations of
291 OK, RK, CK with SOCt as the covariable and CK with NH4Nt and NO3Nt as the covariables

were able to predict that the total amount of N_2O emissions in the tea fields during the wet season were 208.1 g N d^{-1}, 148.2 g N d^{-1}, 149.7 g N d^{-1} and 150.5 g N d^{-1}, respectively. From the performance evaluations of the four spatial interpolations, the total N_2O emissions from the tea field on 22 April 2012 during the wet season were approximately 150 g N d^{-1}.

<Insert Fig. 10 near here>

Discussion

4.1 *Seasonal differences of N_2O fluxes in the red soil planted with tea*

The N_2O emissions from soils have obvious seasonal fluctuations, with emissions that are significantly higher during the wet season than during the dry season (Konda et al., 2010). To understand the seasonal changes in the spatial structures of N_2O fluxes, we compared the N_2O emissions between the wet (this study) and dry (Li et al., 2013) seasons. In general, the mean, SD and coefficient of variation (102.24, 239.96 g N ha^{-1} d^{-1} and 234.7 %, respectively) of the N_2O fluxes in the wet season were all higher than those (2.88, 8.94 g N ha^{-1} d^{-1} and 152.0 %, respectively) during the dry season (Table 3). Furthermore, in contrast with the dry season, the N_2O fluxes during the wet season were significantly different among the four chamber placement positions, with the highest fluxes occurring at the fertilization points and the inter-row positions (Table 3). During the wet season, the high N_2O fluxes at the fertilization points and the inter-row positions resulted from the high soil moisture, due to more rainfall, and from the fertilization that occurred on 19 February 2012 (Fig. 2). The soil N and the soil organic C availability are directly increased by the application of chemical and

organic N fertilizers. The additional in the available C and N supplied by fertilization resulted in increased soil microbial activity, which stimulated the nitrification and denitrification processes that contribute to soil N_2O emissions (Davidson et al., 1993; Kiese et al., 2003; Werner et al., 2007).

<Insert Table 3 near here>

4.2 *Spatial structure of N_2O emissions from red soils planted with tea*

Soil type, topography and land management (fertilization, tillage and irrigation) are the primary factors that affect the spatial structures of N_2O emissions (Folorunso and Rolston, 1984; Clemens et al., 1990; Velthof et al., 1996; Konda et al., 2008). During the wet season, the N_2O fluxes showed a strong spatial dependence (with a range of approximately 25.3 m) that was similar to the dry season range of approximately 28.0 m in the tea-planted fields (Li et al., 2013). These results indicated that the spatial dependence of N_2O fluxes at the current spatial sampling scale was comparable between seasons. Our findings for a fertilized tea field were similar to those of Konda et al. (2010) for a tropical forest. However, these results contrasted those of many previous investigations for agricultural fields, including winter wheat (Ball et al., 1997; Clemens et al., 1999; Röver et al., 1999; Mathieu et al., 2006), summer maize (Clements et al., 1999), onion (Yanai et al., 2003), and grassland (Ambus and Christensen, 1994; Velthof et al., 1996; van den Pol-van Dasselaar et al., 1998; Turner et al., 2008) fields, in which the N_2O flux presented no, weak or moderate spatial dependence. This

discrepancy primarily occurred because of the unique geographical characterization and land management of the tea plantation. Compared with other agricultural fields in flat areas, tea fields are always distributed in hills or mountains. Therefore, the contributions of the topography to the spatial dependence of the N_2O flux were strong (Li et al., 2013). Additionally, tea is a perennial plant. Thus, apart from fertilization and weeding, the soil disturbance in tea fields is always very low.

During the dry season, the topography (elevation) had a significant effect on the spatial pattern of N_2O fluxes in the tea-planted fields (Li et al., 2013). Similar spatial patterns of N_2O fluxes with topography were also observed in forest soils (Van Kessel et al., 1993; Konda et al., 2010). Theoretically, the SWC varies with the topography and affects the spatial pattern of N_2O fluxes by controlling the conditions for soil nitrification and denitrification (Firestone and Davidson, 1989; Wrage et al., 2004). Although the SWC had no relationships with N_2O and elevation during the dry season (Li et al., 2013), a correlation existed in the present study (Fig. 5). The microstructures of the tea tree-row transect and the land management practices of tea production were the primary influences on the spatial pattern of soil water in the tea-planted fields (Li et al., 2013). During the wet season, fertilization contributed to the spatial pattern of N_2O fluxes in the tea-planted fields, with the highest averaged fluxes at the fertilization sites (198.81 g N ha^{-1} d^{-1}) (Table 3). Fertilization resulted in similar spatial patterns of N_2O fluxes in other agricultural soils (Ball et al., 1997; Clements et al., 1999; Röver et al., 1999; Mathieu et al., 2006; Yanai et al., 2003).

In view of the analysis of the primary factors that affected the spatial pattern of N_2O fluxes, we detrended the influences of the environmental factors when the N_2O flux semivariograms were calculated to more deeply explore the spatial structures of the N_2O emissions in the tea-planted fields. For example, during the dry and wet seasons, the spatial influences of elevation (Li et al., 2013) and chamber placement position, respectively, were detrended when computing the N_2O flux semivariograms. Because the relationship between chamber placement position and N_2O flux was more relevant than the relationship between elevation and N_2O flux, the effect of detrending the influence of chamber placement position during the wet season was more obvious than that of detrending the influence of elevation during the dry season (Li et al., 2013). This effect was also reflected in the evaluation of the performance of the RK method for the wet and dry seasons (Table 4).

4.3 Spatial interpolations of N_2O emissions by three methods

The three interpolation methods (OK, RK and CK) were used to predict the spatial distributions of N_2O emissions from the red soils planted with tea during dry (Li et al., 2013) and wet seasons (this study). However, these three methods resulted in significantly different performances between the dry and wet seasons (Table 4). We conducted comparative analyses for the performance of the three interpolation methods using two aspects: different seasons and different methods. Firstly, the OK method performed better when predicting the spatial distribution of N_2O fluxes for the dry season relative to the wet season. Because the OK method directly used the fitted theoretical semivariogram model of the target variable to

predict the spatial distribution, its performance reflected the predictive ability of the original data (Goovaerts, 1997). During the wet season, more factors (e.g., NH4N, NO3N, SOC, TSN and SWC) influenced the spatial distributions of the N_2O fluxes than the dry season (Table 2 and Fig. 5). The values of the original data were concealed. Thus, other sophisticated kriging methods, such as RK and CK, which reconcile the relationships between N_2O fluxes and environmental factors, could be useful. The RK method performed better when elevation was used as an auxiliary regression predictor during the dry season than when the chamber placement position was used during the wet season (Table 4). This finding primarily occurred because the chamber placement position was a categorical variable with a lower regression fitting ability than elevation, which was a continuous variable (Goovaerts, 1997). The performances of the CK with two groups of covariables during the wet season were better than those of the CK with three groups of covariables during the dry season (Table 4). Particularly, the CK with strongly correlated covariables of NO3N and NH4N (r = 0.70-0.71 and $p < 0.001$) (Fig. 5) performed the best (r = 0.74 and RMSE = 1.04) (Table 4).

Secondly, by comparing the performances of the three interpolation methods, the RK and CK methods, which are more sophisticated kriging technologies, performed better than the OK method for the dry and wet seasons. Similar results were obtained by previous researchers (Stein et al., 1988; Odeh et al., 1995; Goovaerts, 1997; Hengl et al., 2004).When comparing the performances of RK and CK, no differences were observed for the dry season. However, during the wet season, the CK significantly outperformed the RK (Table 4). Overall, few attempts have been made to provide a good method for selecting interpolation methods

between RK and CK (Kontters et al., 1995; Odeh et al. 1995). Li et al. (2013) suggested that RK was a good choice because of the performance of the two interpolation methods and the difficulties encountered when applying CK. However, in this study, the CK method was better than the RK method because of its high predictive performance (Table 4), its readily available required covariables (e.g., NH4N, NO3N and SOC) at co-locations, and because expensive surface data were not needed (e.g., DEM and land use data, which are required by RK) (Goovaerts, 1997; Webster and Oliver, 2001). Our conclusions were similar to those of many previous studies that found that CK was the most versatile and rigorous statistical technique for estimating spatial points (Stein et al., 1988; Odeh et al., 1995; Webster and Oliver, 2001). For the application of CK, the covariables must show a correlation with the target variable and present a similar spatial structure as the target variable (Odeh et al., 1995; Goovaerts, 1997; Webster and Oliver, 2001). Therefore, we further compared the effects of the two groups of covariables for CK in this study. We found that CK method with NH4Nt and NO3Nt (showed significant correlations with FLUX30t) as covariables outperformed the CK method with SOCt (presented a similar spatial structure to FLUX30t) as a covariable, indicating that the feature correlation was more important than the similarity of the spatial structure when selecting CK covariables. This finding can be regarded as a prerequisite for selecting covariables for CK application.

<Insert Table 4 near here>

418 The three spatial interpolation methods predicted similar total N_2O emissions from the
419 tea-planted red soils in the 4.0 ha catchment on 30 October 2010 (in the dry season) and on
420 22 April 2012 (in the wet season), ranging from 21.2 to 22.1 g N d^{-1} and from 148.2 to 208.1
421 g N d^{-1} (Table 4), respectively. The predicted errors during the wet season were higher than
422 those of the dry season (Table 4). This result mainly occurred because fertilization was a
423 major factor that affected the N_2O emissions from the tea fields during the wet season.
424 Following fertilization, the horizontal and vertical movement of NH4N and NO3N in the
425 topsoil of the tea fields potentially produced the strong spatial heterogeneity of N_2O
426 emissions. In addition, it is possible that the variations in the availability of oxygen in the
427 soils was regulated by soil moisture, which determined the spatio-temporal heterogeneity of
428 N_2O emissions by inducing different degrees of soil nitrification and denitrification
429 (Davidson et al., 2000; Konda et al., 2010). Thus, spatial interpolation methods must be
430 chosen carefully to accurately estimate the spatial distribution of N_2O emissions when the
431 emissions are high and have strong spatial variability in the fields.
432
433 **5 Conclusions**
434 During the wet season of 2012, a 30-min one-time measurement of N_2O emissions from a 4.0
435 ha red-soil tea field in the subtropical region of central China were determined at 147 points.
436 The N_2O fluxes significantly varied with space. In addition, the N_2O fluxes were significantly
437 correlated with the NH4N, NO3N, SOC and TSN contents ($r > 0.27$ and $p < 0.001$). The
438 logit-transformed N_2O fluxes demonstrated a strong spatial dependency and were

characterized by an exponential semivariogram model with an effective range of 25.2 m. Three spatial interpolation methods (OK, RK and CK) were used to predict the spatial distribution of N_2O emissions. The RK and CK methods were relatively accurate for predicting results. Although the N_2O emissions were much higher during the wet season than in the dry season, the N_2O emissions exhibited similar spatial structure during both seasons. Such a phenomenon was mainly attributed to the low soil disturbance (e.g., only fertilizing in a very small proportion of area and weeding) in the tea field.

To effectively mitigate high N_2O emissions from the tea field soils, the biological and chemical mechanisms of N_2O emissions must be deeply explored. In addition, the responsive land management practices, such as biochar application, deep fertilization (under 20 cm), the use of controlled-release fertilizers and ecological engineering, must be recommended and deployed, especially during the wet season.

Acknowledgements

The National Basic Research Program of China (2012CB417105) and the National Natural Science Foundation of China (41171200) financially supported this research.

References

Akiyama, H., Yan, X. Y., and Yagi, K.: Estimations of emission factors for fertilizer-induced direct N_2O emissions from agricultural soils in Japan: Summary of available data, Soil Sci. Plant Nutr., 52, 774-787, 2006.

Ambus, P. and Christensen, S.: Measurement of N_2O emission from a fertilized grassland: an analysis of spatial variability, J. Geophys. Res., 99, 16557-16567, 1994.

Armstrong, M.: Basic linear Geostatistics, Springer Verlag, Berlin, 153 pp., 1998.

Ball, B. C., Horgan, G. W., Clayton, H., and Parker, J. P.: Spatial variability of nitrous oxide fluxes and controlling soil and topographic properties, J. Environ. Qual., 26, 1399-1409, 1997.

Clemens, J. Schillinger, M. P., Goldbach, H., and Huwe, B.: Spatial variability of N_2O emissions and soil parameters of an arable silt loam - a field study, Bio. Fert. Soils, 28, 403-406, 1999.

Davidson, E. A., Matson, P. A., Vitousek, P. M., Riley, R., Dunkin, K., García-Méndez, G., and Maass, J. M.: Processes regulating soil emissions of NO and N_2O in a seasonally dry tropical forest, Ecology, 74, 130-139, 1993.

Davidson, E. A., Keller, M., Erickson, H. E., Verchot, L. V., and Veldkamp, E.: Testing a conceptual model of soil emissions of nitrous and nitric oxides, Bioscience, 50, 667-680, 2000.

DGUU (Department of Geography, Utrecht University): Introduction for Gstat, available at: http://www.gstat.org/index.html (last access: 15 December 2010), 2010.

476 Firestone, M., and Davidson, E.: Microbial basis of NO and N_2O production and
477 consumption, in: Exchange of Trace Gases Between Ecosystems and the Atmosphere,
478 edited by: Andreae, M.O. and Schimel, D.S., John Wiley, Chichester, 7-21, 1989.
479 Folorunso, O. A., and Rolston, D. E.: Spatial variability of field measured denitrification gas
480 fluxes, Soil Sci. Soc. Am. J., 48, 1214-1219, 1984.
481 Fu, X., Li, Y., Xiao, R., Tong, C., and Wu, J.: N_2O emissions from a tea field in subtropical
482 China. In: Proceedings of the 19th World Congress of Soil Science, Soil Solutions for a
483 Changing World, 1–6 August 2010, Brisbane (published on CDROM), 161-163, 2010.
484 Fu, X., Li, Y., Su, W., Shen, J., Xiao, R., Tong, C., and Wu, J.: Annual dynamics of N2O
485 emissions from a tea field in southern subtropical China, Plant Soil Environ., 58,
486 373-378, 2012.
487 Goovaerts, P.: Geostatistics for Natural Resources Evaluation, Oxford University Press, New
488 York, 483 pp., 1997.
489 Gorres, J. H., Dichiaro, M. J., and Lyons, J. A.: Spatial and temporal patterns of soil
490 biological activity in a forest and an old field, Soil Biol. Biochem., 30, 219-230, 1998.
491 Han, W. Y., Xu, J. M., Wei, K., Shi, W. Z., and Ma, L. F.: Estimation of N_2O emission from
492 tea garden soils, their adjacent vegetable garden and forest soils in eastern China, Environ.
493 Earth Sci., 70, 2495-2500, 2013.
494 Hayatsu, M.: The lowest limit of pH for nitrification in tea soil and isolation of an acidophilic
495 ammonia oxidizing bacterium, Soil. Sci. Plant Nutr., 39, 219-226, 1993.

Hengl, T., Heuvelink, G. B. M., and Stein, A.: A generic framework for spatial prediction of soil variables based on regression-kriging, Geoderma, 120, 75-93, 2004.

Hirono, Y., and Nonaka, K.: Nitrous oxide emissions from green tea fields in Japan: contribution of emissions from soil between rows and soil under the canopy of tea plants, Soil. Sci. Plant Nutr., 58, 384-392, 2012.

IPCC: Climate change 2013: the physical science basis. Contribution of working group I, in: Fourth assessment report of the intergovernmental panel on climate change, edited by: Solomon S., Qin D., Manning, M., Chen Z., Marquis, M., Averyt, K.B., Tignor, M., Miller, H.L., Cambridge University Press, Cambridge, 996 pp., 2013.

ISM (Institute for Statistics and Mathematics): The R Project for Statistical Computing, available at: http://www.r-project.org/ (last access: 15 December 2010), 2010.

Kiese, R., Hewett, B., Graham, A., and Butterbach-Bahl, K.: Seasonal variability of N_2O emissions and CH_4 uptake by tropical rainforest soils of Queensland, Australia. Global Biogeochem. Cy., 17, 1043, doi:10. 1029/2002GB002014, 2003.

Konda, R., Ohta, S., Ishizuka, S., Arai, S., Ansori, S., Tanaka, N., and Hardjono, A.: Spatial structures of N_2O, CO_2, and CH_4 fluxes from Acacia mangium plantation soils during a relatively dry season in Indonesia, Soil Biol. Biochem., 40, 3021-3030, 2008.

Konda, R., Ohta, S., Ishizuka, S., Heriyanto, J., and Wicaksono, A.: Seasonal changes in the spatial structures of N_2O, CO_2 and CH_4 fluxes from Acacia mangium plantation soils in Indonesia, Soil Biol. Biochem., 42, 1512-1522, 2010.

516 Li, Y., Fu, X., Liu, X., Shen, J., Luo, Q., Xiao, R., Li, Y., Tong, C., and Wu, J.: Spatial
517 variability and distribution of N_2O emissions from a tea field during the dry season in
518 subtropical central China, Geoderma, 193, 1-12, 2013.
519 Lin, Y., and Han, W.: N_2O emissions from different soils, Chinese Journal of Tea Science, 29,
520 456-464, 2009.
521 Mathieu, O., Lévêque, J., Hénault, C., Milloux, M. J., Bizouard, F., and Andreux, F.:
522 Emissions and spatial variability of N_2O, N_2 and nitrous oxide mole fraction at the field
523 scale, revealed with ^{15}N isotopic techniques, Soil Biol. Biochem., 38, 941-951, 2006.
524 Meda, B., Flechard, C. R., Germain, K., Robin, P., Walter, C., and Hassouna, M.:
525 Greenhouse gas emissions from the grassy outdoor run of organic broilers,
526 Biogeosciences, 9, 1493-1508, doi:10.5194/bg-9-1493-2012, 2012.
527 Mosier, A. R., Duxbury, J. M., Freney, J. R., Heinemeyer, O., and Minami, K.: Nitrous oxide
528 emissions from agricultural fields: assessment, measurement and mitigation. Plant Soil,
529 181, 95-181, 1996.
530 Mosier, A. R., Kroeze, C., Nevison, C., Oenema, O., Seitzinger, S., and van Cleamput, O.:
531 Closing the global N_2O budget: nitrous oxide emissions through the agricultural nitrogen
532 cycle, Nutr. Cycl. Agroecosys., 52, 225-248, 1998.
533 NBSC (a): China Statistical Yearbook, annual publication, National Bureau of Statistics of
534 China, Beijing, 2014.

Odeh, I. O. A., McBratney, A. B., and Chittleborough, D. J.: Spatial prediction of soil properties from landform attributes derived from a digital elevation model, Geoderma, 63, 197-214, 1994.

Odeh, I. O. A., McBratney, A. B., and Chittleborough, D. J.: Further results on prediction of soil properties from terrain attributes: heterotopic cokriging and regression kriging, Geoderma, 67, 215-226, 1995.

R Development Core Team: R: a language and environment for statistical computing. R Foundation for Statistical Computing, 2014.

Ravishankara, A. R., Daniel, J. S., and Portmann, R. W.: Nitrous oxide (N_2O): the dominant ozone-depleting substance emitted in the 21st century, Science, 326, 123-125, 2009.

Röver, M., Heinemeyer, O., Munch, J. C., and Kaiser, E. A.: Spatial heterogeneity within the plough layer: high variability of N_2O emission rates, Soil Biol. Biochem., 31, 167-173, 1999.

Stein, A., van Dooremolen, W., Bouma, J., and Bregt, A. K.: Cokriging point data on moisture deficit. Soil Sci. Soc. Am. J., 52, 1418-1423, 1988.

Tokuda, S. I., and Hayatsu, M.: Nitrous oxide flux from a large amount of nitrogen fertilizer and soil environmental factors controlling the flux, Soil. Sci. Plant Nutr., 50, 365-374, 2004.

Turner, D. A., Chen, D., Gellbally, I. E., Li, Y., Edis, R. B., Leuning, R., Kelly, K., and Phillips, F.: Spatial variability of nitrous oxide emissions from an Australian irrigated dairy pasture, Plant soil, 309, 77-88, 2008.

Van den Pol-van Dasselaar, A., Corré, W. J., Klemedtsson, A., Weslien, P., Stein, A., Klemedtsson, L., and Oenema, O.: Spatial variability of methane, nitrous oxide, and carbon dioxide emissions from drained grasslands, Soil Sci. Soc. Am. J., 62, 810-817, 1998.

Van Kessel, C., Pennock, D.J., and Farrell, R.E.: Seasonal-variations in denitrification and nitrous oxide evolution at the landscape scale, Soil Sci. Soc. Am. J., 57, 988-995, 1993.

Velthof, G. L., Jarvis, S. C., Stein, A., Allen, A. G., and Oenema, O.: Spatial variability of nitrous oxide fluxes in mown and grazed grasslands on a poorly drained clay soil, Soil Biol. Biochem., 28, 1215-1225, 1996.

Venterea, R. T., and Rolston, D. E.: Mechanisms and kinetics of nitric and nitrous oxide production during nitrification in agricultural soil, Glob. Change Biol., 6, 303-316, 2000.

Webster, R.: Quantitative spatial analysis of soil in the field, in: Advances in Soil Science, edited by: Stewart, B.A., Springer, New York, 1-70, 1985.

Webster, R., and Oliver, M. A.: Geostatistics for Environmental Scientists, John Wiley & Sons, Chichester, 2001.

Werner, C., Kiese, R., and Butterbach-Bahl, K.: Soil-atmosphere exchange of N_2O, CH_4, and CO_2 and controlling environmental factors for tropical rain forest sites in western Kenya, J. Geophys Res., 112, D03308, doi:10.1029/2006JD007388, 2007.

Wrage, N., Velthof, G. L., Laanbroek, H. J., and Oenema, O.: Nitrous oxide production in grassland soils: assessing the contribution of nitrifier denitrification, Soil Biol. Biochem., 36, 229-236, 2004.

577 Yanai, J., Lee, C. K., Umeda, M., and Kosaki, T.: Spatial variability of soil chemical
578 properties in a paddy field. Soil Sci. Plant Nutr., 46, 473-482, 2000.
579 Yanai, J., Sawamoto, T., Oe, T., Kusa, K., Yamakawa, K., Sakamoto, K., Naganawa, T.,
580 Inubushi, K., Hatano, R., and Kosaki, T.: Atmospheric pollutants and trace gases: spatial
581 variability of nitrous oxide emissions and their soil-related determining factors in an
582 agricultural field, J. Environ. Qual., 32, 1965-1977, 2003.
583

584 Table 1 Descriptive statistics of the N_2O fluxes and environmental factors.

Variable[a]	Mean	Minimum	Maximum	CV (%)	Skewness of the original data	Skewness of the logit-transformed data
FLUX30	102.24[b]	-1.73	1,659.11	234.7	4.37	0.6
ELEVATION	80.64	74.25	87.96	4.1	0.04	-
BD	1.26	0.90	1.56	10.1	-0.28	-
DOC	185.56	43.70	424.14	34.6	0.75	-
NH4N	62.33	1.89	842.55	190.8	3.28	0.17
NO3N	21.54	0.48	135.29	141.6	1.85	0.28
SOC	13.33	5.11	52.52	50.1	2.27	-0.44
TSN	1.52	0.81	4.12	38.3	1.73	-0.01
SWC	0.33	0.19	0.47	16.6	0.07	-
SAND	39.73	16.98	63.79	23.8	0.02	-
SILT	47.15	26.78	64.17	16.1	-0.29	-
CLAY	13.12	8.68	21.68	21.5	1.00	-

585 [a]FLUX30 is the N_2O flux (g N ha^{-1} d^{-1}); ELEVATION is the elevation (m); and BD, DOC,
586 NH4N, NO3N, SOC, TSN, SWC, SAND, SILT and CLAY are the soil bulk density (Mg m^{-3}),
587 soil dissolved organic carbon (mg C kg^{-1} soil), soil ammonium (mg N kg^{-1} soil), soil nitrate
588 (mg N kg^{-1} soil), soil organic carbon (g C kg^{-1} soil), soil total nitrogen (g N kg^{-1} soil),

589 gravimetric soil water (g H_2O g^{-1} soil), soil sand particle (%), soil silt particle (%) and soil

590 clay particle (%) content, respectively, of the 0-20 cm of topsoil.

591 [b]The median and standard deviation of the FLUX30 were 27.56 and 239.96 g N ha^{-1} d^{-1},

592 respectively.

593 Table 2 Semivariogram models for N_2O fluxes and the environmental factors.

Variable	Model	Nugget	Partial sill	Sill(nugget+ partial sill)	Distance Parameter (m)	Effective range (m)	Partial sill/sill
FLUX30t[a]	Exp	0	3.7186	3.7186	8.40	25.2	1.00
NH4Nt[a]	ND[c]	ND[c]	ND[c]	ND[c]	ND[c]	ND[c]	ND[c]
NO3Nt[a]	Ste	4.0794	0.6113	4.6907	91.92	163.7	0.13
SOCt[a]	Sph	1.1198	0.7744	1.8942	92.96	93.0	0.41
TSNt[a]	Ste	1.0422	0.2816	1.3238	57.97	102.6	0.21
SWCt[a]	ND[c]	ND[c]	ND[c]	ND[c]	ND[c]	ND[c]	ND[c]
SAND[a]	ND[c]	ND[c]	ND[c]	ND[c]	ND[c]	ND[c]	ND[c]
SILT[a]	ND[c]	ND[c]	ND[c]	ND[c]	ND[c]	ND[c]	ND[c]
FLUX30t[b]	Exp	1.1911	2.0560	3.2471	17.36	52.1	0.63
NH4Nt[b]	Exp	2.0473	0.7185	2.7658	17.36	52.1	0.26
NO3Nt[b]	Exp	1.6241	1.1188	2.7429	17.36	52.1	0.41
SOCt[b]	Exp	0.6043	1.0777	1.6820	17.36	52.1	0.64
TSNt[b]	Ste	0.9347	0.3114	1.2461	59.53	105.4	0.25
SWCt[b]	ND[c]	ND[c]	ND[c]	ND[c]	ND[c]	ND[c]	ND[c]
SAND[b]	ND	ND	ND	ND	ND	ND	ND
SILT[b]	ND	ND	ND	ND	ND	ND	ND

594 ND, not determined.

595 [a]Semivariogram models for the OK method.

[b]Semivariogram models for the RK method using the chamber placement position as the auxiliary regression predictor.

[c]Spatial structures were not apparent.

600 Table 3 Statistics for N_2O fluxes during the dry and wet seasons.

Sample position	Mean	SD	Median	Max.	Min.	CV (%)
Dry season						
Inter-row (58)	5.15	4.95	4.09	22.43	-2.83	96.1
Fertilization point (50)	7.19	12.04	4.34	79.56	-6.42	167.4
Under tree (28)	3.58	2.91	2.36	10.28	0.68	81.3
In tree row (11)	5.95	10.38	3.98	52.17	-5.69	174.5
Wet season						
Inter-row (45)	101.69	287.23	27.56	1,659.11	-0.81	282.5
Fertilization point (45)	198.81	295.70	73.42	1,404.32	0.85	148.7
Under tree (22)	16.74	17.00	10.64	61.24	-1.73	101.6
In tree row (33)	28.30	38.34	14.72	177.08	0.19	135.5

601 The numbers in the parentheses represent the sample numbers for each chamber placement
602 position.
603

Table 4 Cross-validations of the three different kriging interpolations for N_2O fluxes during the dry and wet seasons.

Method of spatial interpolation	Auxiliary variable	ME (no dimension)	RMSE (no dimension)	*r*	Predicted total N_2O emissions (g N d^{-1})
Dry season					
OK	-	0.0002	0.102	0.52	22.1[a]
RK	ELEVATION	0.0008	0.098	0.57	21.1[a]
CK	SOCt	0.0006	0.103	0.51	22.0[a]
CK	ELEV	0.0008	0.099	0.57	21.5[a]
CK	SOCt and ELEV	0.0009	0.098	0.57	21.2[a]
Wet season					
OK	-	-0.0005	1.739	0.18	208.1
RK	POSITION	-0.0006	1.549	0.49	148.2
CK	SOCt (POSITION)	0.0020	1.439	0.58	149.5
CK	NH4Nt (POSITION) and NO3Nt (POSITION)	0.0001	1.185	0.74	150.5

606 OK, RK and CK correspond to ordinary kriging, regression kriging and cokriging,
607 respectively; For the dry season campaign, ELEVATION, SOCt and ELEV are the normalized
608 elevation, the normalized soil organic carbon content and the inverse of the normalized
609 elevation, respectively. For the wet season campaign, SOCt, NH4Nt and NO3Nt are the
610 logit-transformations of soil organic carbon, soil ammonium and soil nitrate concentrations,
611 respectively. "POSITION" (in the parentheses) indicates the process of detrending the
612 influence of chamber placement position. The ME, RMSE, and r are the mean prediction
613 error, the root mean squared error (the mean squared deviation ratio of the prediction
614 residuals to the kriging standard errors), and the Pearson's correlation coefficient between the
615 observations and the predictions, respectively.
616 [a]The predicted total N_2O emissions during the dry season were recalculated because the study
617 area changed from 4.8 ha to 4.0 ha for the wet season.
618

Figure captions

Figure 1. (**a, b**) Location and (**c, d**) digital elevation model and land use map of the tea planted catchment. The red circles in (**c, d**) represent the sample points. The catchment is located in Jinjing town, which is 70 km northeast of Changsha, the capital city of Hunan Province, China.

Figure 2. Daily (**a**) air temperatures and (**b**) precipitation during 2012.

Figure 3. Histograms of (**a**) the original N_2O fluxes (FLUX30) and (**b**) the logit-transformed N_2O fluxes (FLUX30t).

Figure 4. The Tukey's Honest Significant Difference analysis for FLUX30t, NH4Nt, NO3Nt, SOCt, TSNt and SWCt based on the four-chamber placement positions (R, inter-row; F, fertilization point; U, under tea tree; and I, in the tea tree row).

Figure 5. Correlation matrix with the Pearson's correlation coefficients (r) of the N_2O fluxes and the environmental factors. All of the variables in the correlation matrix are normally distributed. FLUX30 represents the N_2O flux (g N ha^{-1} d^{-1}); ELEVATION is the elevation (m); and BD, DOC, NH4N, NO3N, SOC, TSN, SWC, SAND, SILT and CLAY are the soil bulk density (Mg m^{-3}), soil dissolved organic carbon (mg C kg^{-1} soil), soil ammonium (mg N kg^{-1}

640 soil), soil nitrate (mg N kg^{-1} soil), soil organic carbon (g C kg^{-1} soil), total soil nitrogen (g N
641 kg^{-1} soil), gravimetric soil water (g H_2O g^{-1} soil), soil sand particle (%), soil silt particle (%)
642 and soil clay particle (%) contents of the top 0-20 cm of the soil, respectively. Furthermore, *,
643 ** and *** represent the statistical significance at probability levels of 0.05, 0.01 and 0.001,
644 respectively. The lowercase letter t represents the logit transformation.
645
646 Figure 6. Semivariograms (open circles) and best-fitted models (solid lines) of the normal
647 logit-transformed N_2O fluxes (FLUX30t) (no dimension) for ordinary kriging (**a**) and the
648 regression residuals of FLUX30t (no dimension) with chamber placement position as the
649 predictor for regression kriging (**b**).
650
651 Figure 7. Direct and cross-semivariograms (open circles, detrending the influence of chamber
652 placement position for cokriging) and the best-fitted linear model of the co-regionalization
653 (solid lines) of the normal logit-transformed N_2O fluxes (FLUX30t) (no dimension) and the
654 normal SOC (SOCt, no dimension). The linear model of co-regionalization was characterized
655 by using the same range and different sills for its component models.
656
657 Figure 8. Direct and cross-semivariograms (open circles, detrending the influence of chamber
658 placement position for cokriging) and the best-fit linear model of co-regionalization (solid
659 lines) for the normal logit-transformed N_2O fluxes (FLUX30t) (no dimension), NH4N
660 (NH4Nt, no dimension) and NO3N (NO3Nt, no dimension). The linear model of

661 co-regionalization was characterized by the same range and different sills for its component
662 models.
663
664 Figure 9. Spatial distributions of the N_2O fluxes as predicted by (**a**) OK, (**b**) RK with
665 chamber placement position as the regression predictor, (**c**) CK with SOCt (with the influence
666 of chamber placement position detrended) as the covariable, and (**d**) CK with NH4Nt (with
667 the influence of chamber placement position detrended) and NO3Nt (with the influence of
668 chamber placement position detrended) as two covariables. Here, SOCt, NH4Nt and NO3Nt
669 represent the logit-transformed soil organic carbon, soil ammonium and soil nitrate content,
670 respectively.
671
672 Figure 10. Spatial distributions of kriging standard deviations of the predicted N_2O fluxes by
673 (**a**) OK, (**b**) RK, (**c**) CK with SOCt as the covariable, and (**d**) CK with NH4Nt and NO3Nt as
674 two covariables.

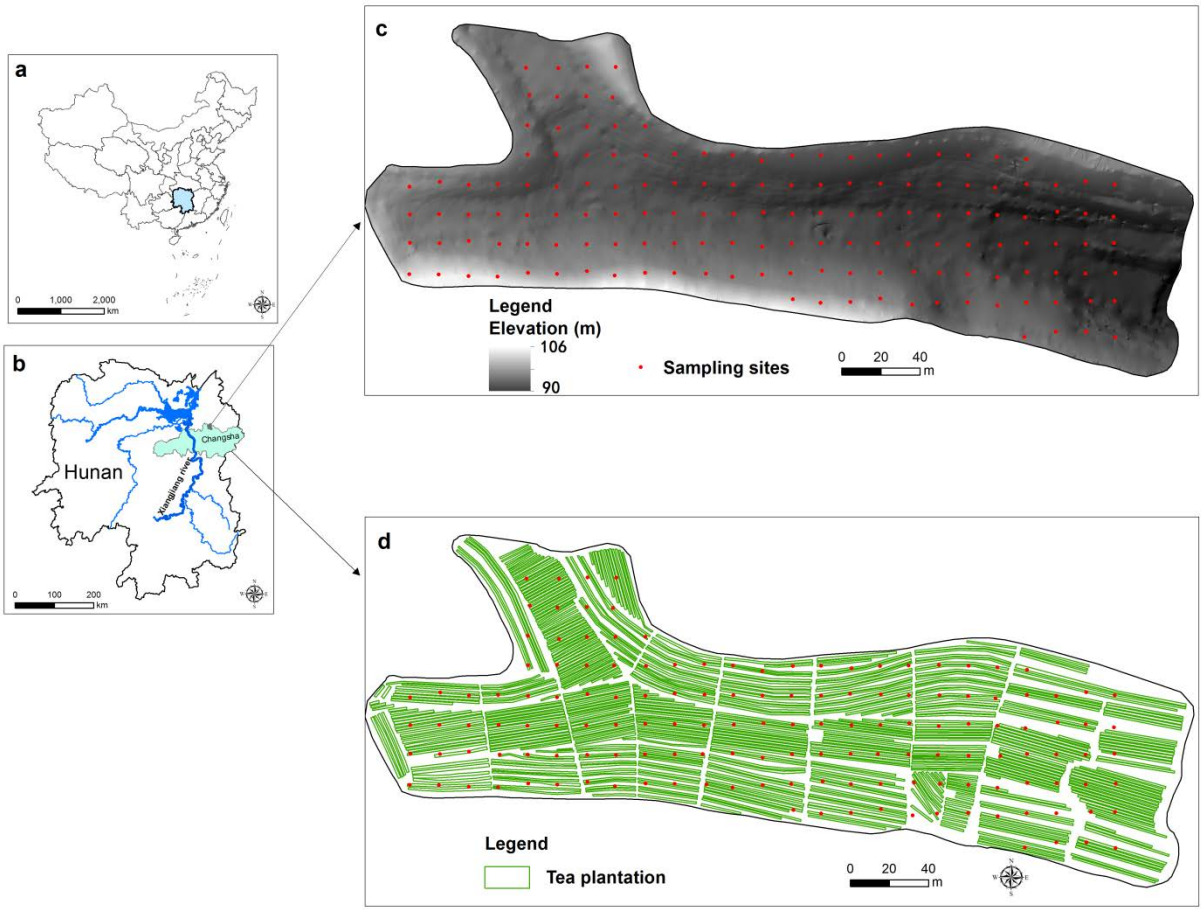

675

676 Figure 1

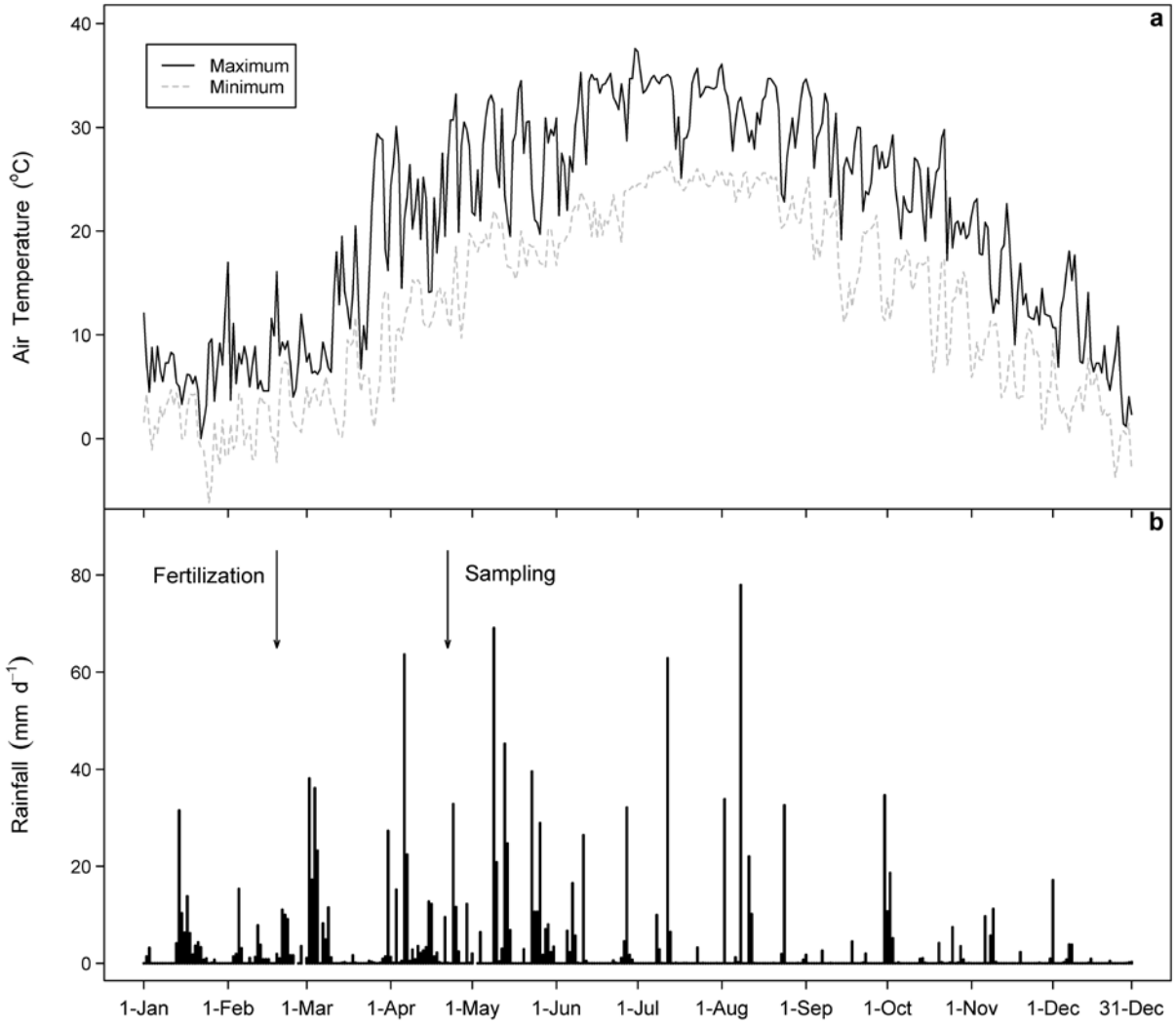

677

678 Figure 2

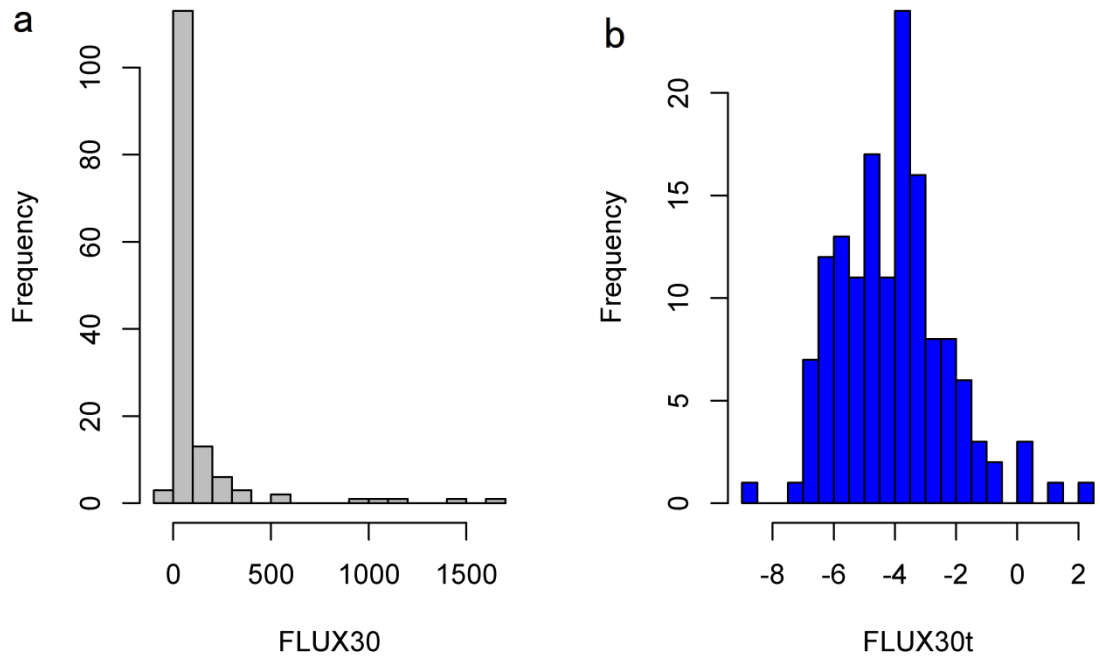

679

680 Figure 3

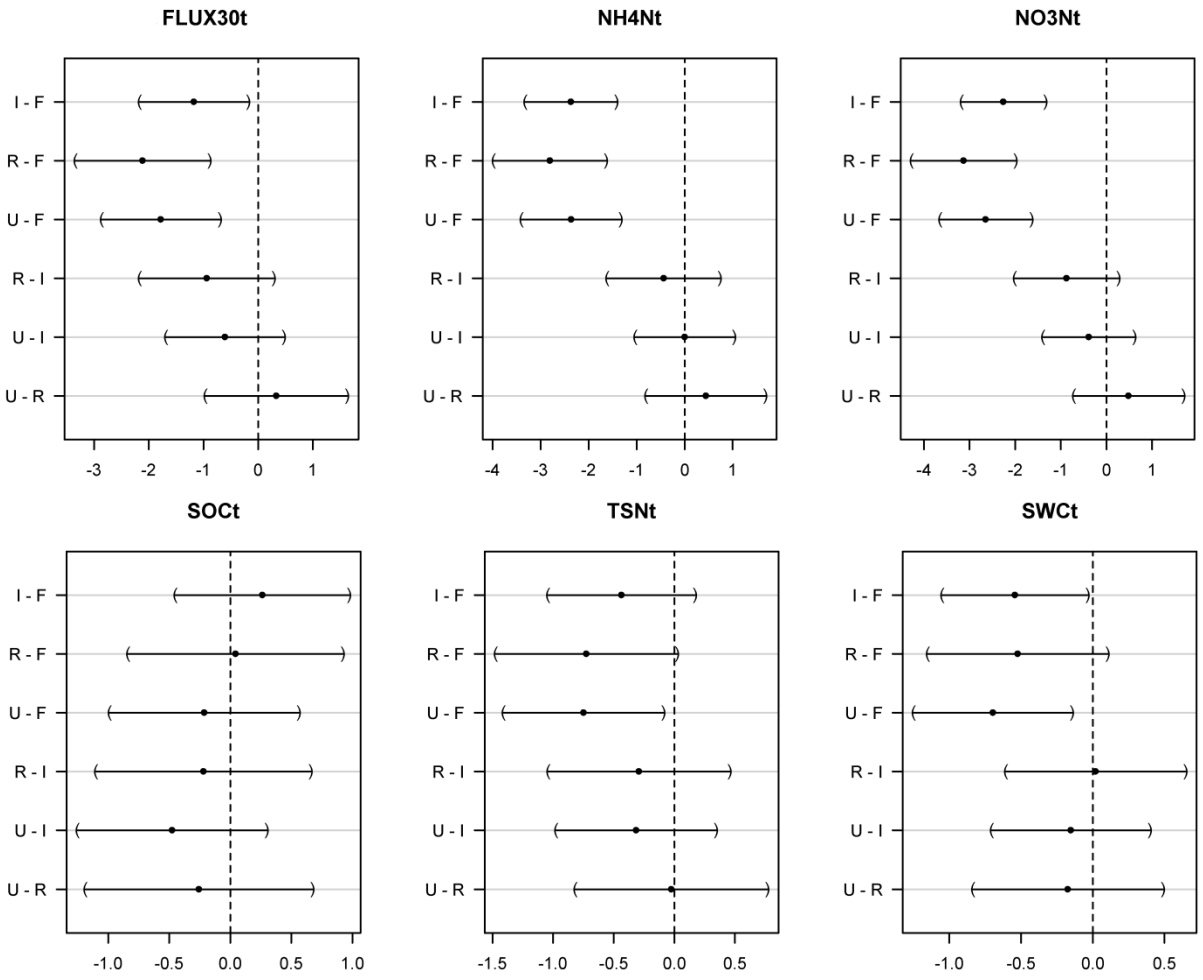

681

682 Figure 4

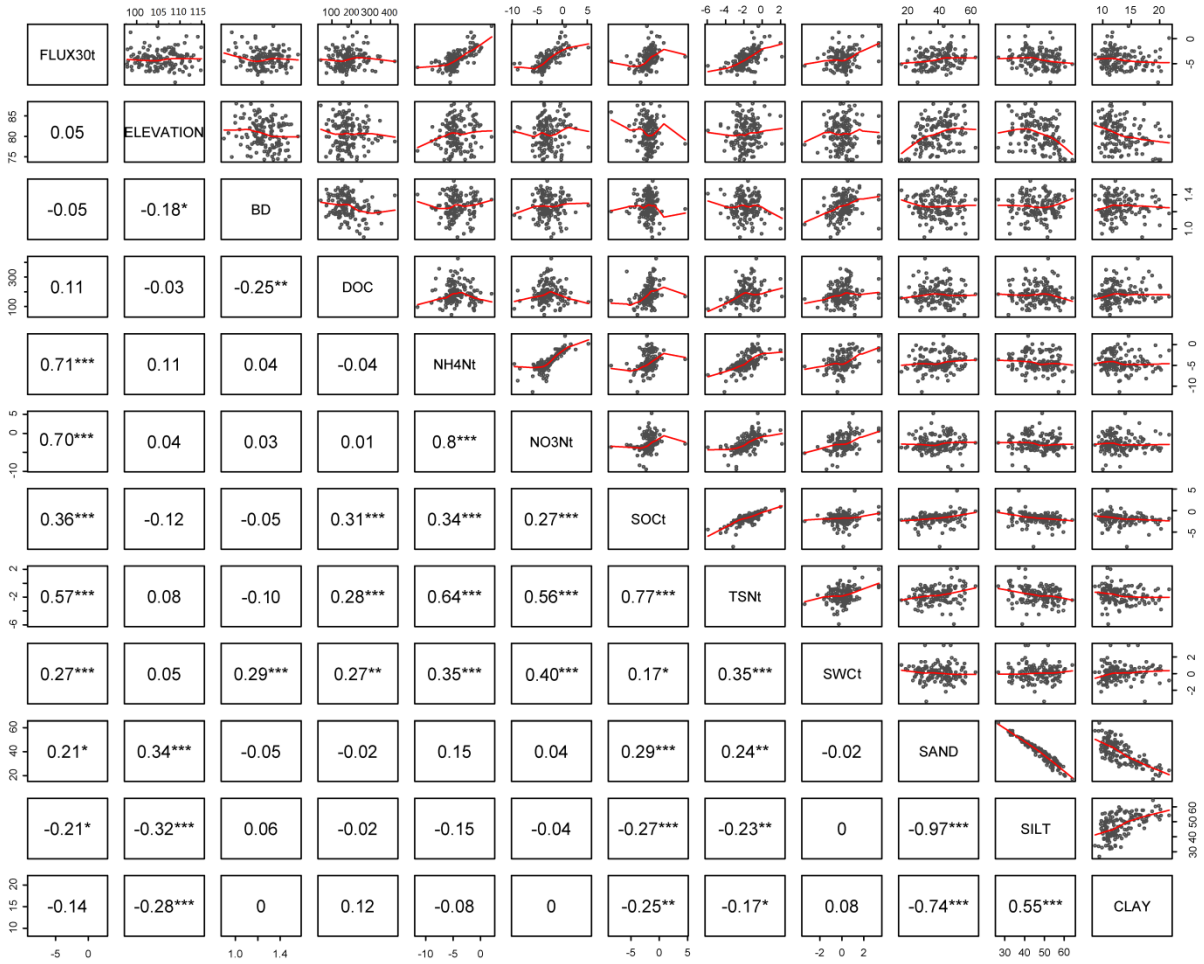
FLUX30t
ELEVATION
BD
DOC
NH4Nt
NO3Nt
SOCt
TSNt
SWCt
SAND
SILT
CLAY
0.05
-0.05
-0.18*
0.11
-0.03
-0.25**
0.71***
0.11
0.04
-0.04
0.70***
0.04
0.03
0.01
0.8***
0.36***
-0.12
-0.05
0.31***
0.34***
0.27***
0.57***
0.08
-0.10
0.28***
0.64***
0.56***
0.77***
0.27***
0.05
0.29***
0.27**
0.35***
0.40***
0.17*
0.35***
0.21*
0.34***
-0.05
-0.02
0.15
0.04
0.29***
0.24**
-0.02
-0.21*
-0.32***
0.06
-0.02
-0.15
-0.04
-0.27***
-0.23**
0
-0.97***
-0.14
-0.28***
0
0.12
-0.08
0
-0.25**
-0.17*
0.08
-0.74***
0.55***

Figure 5

685

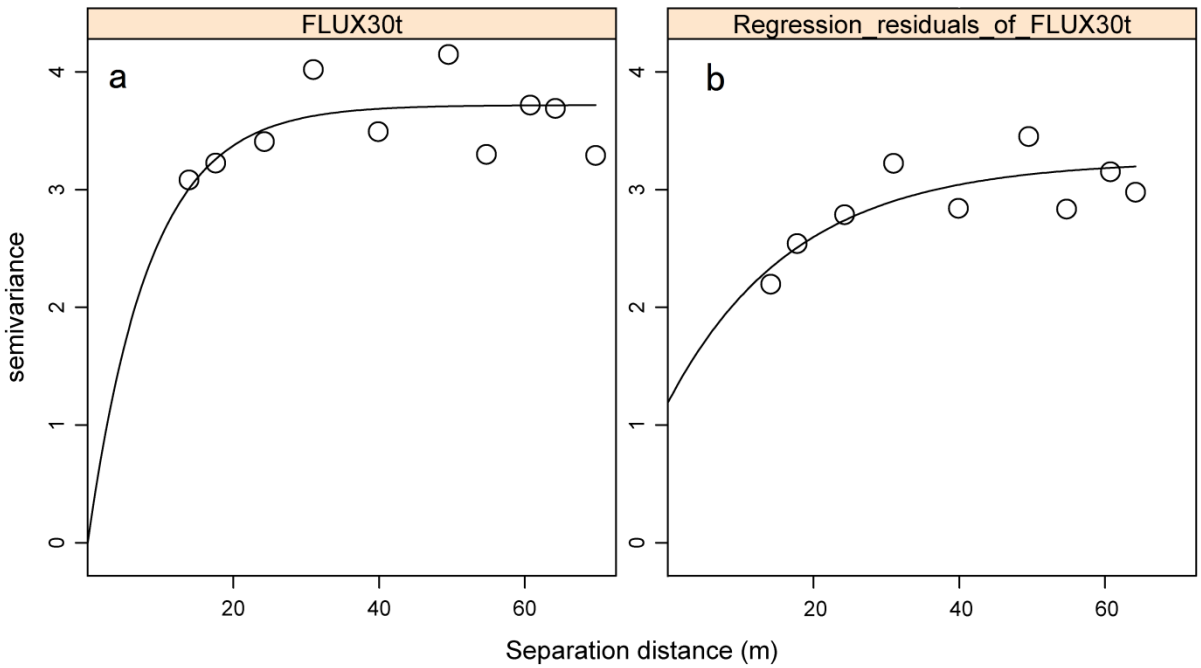

686

687 Figure 6

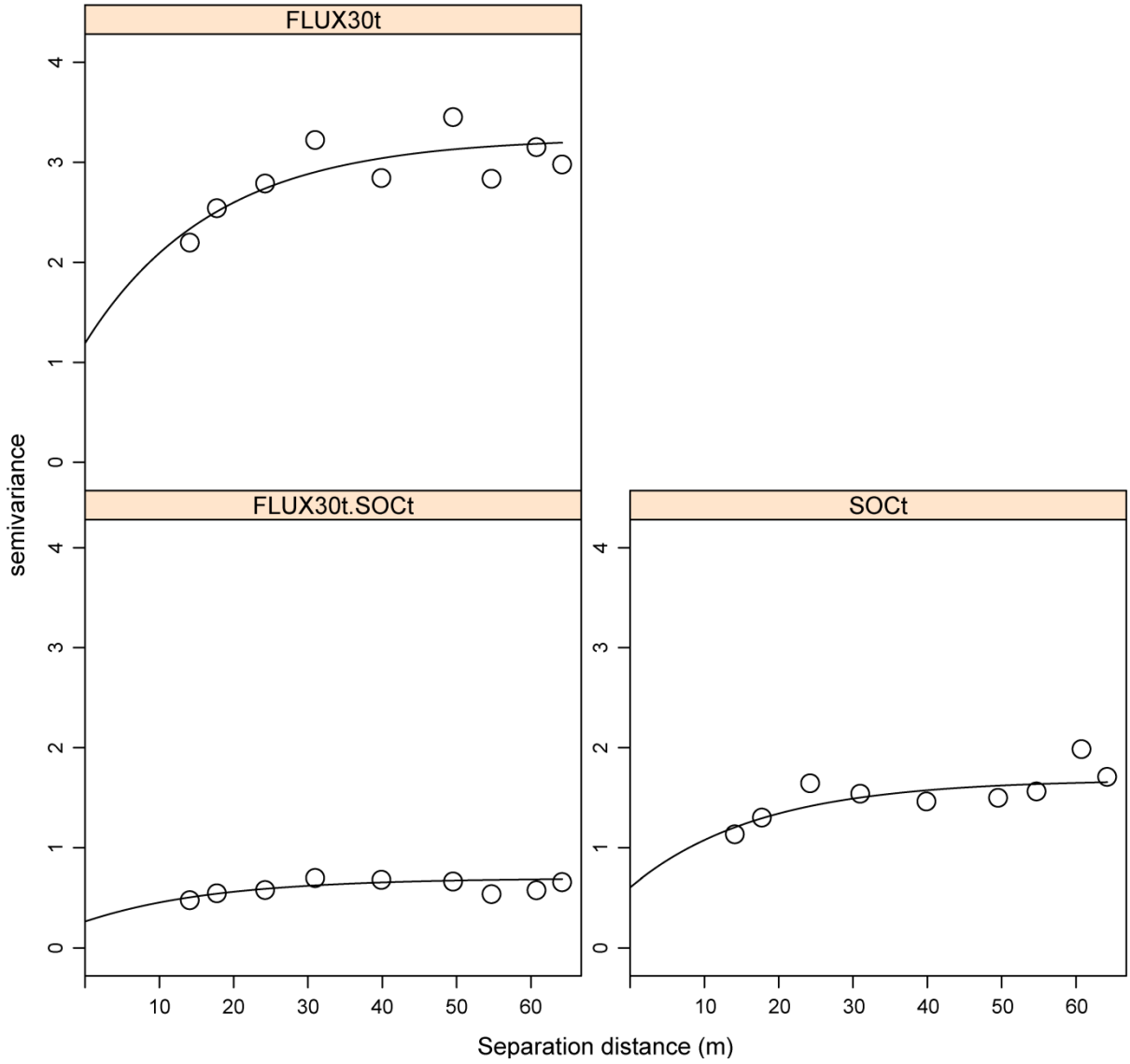

688

689 Figure 7

690

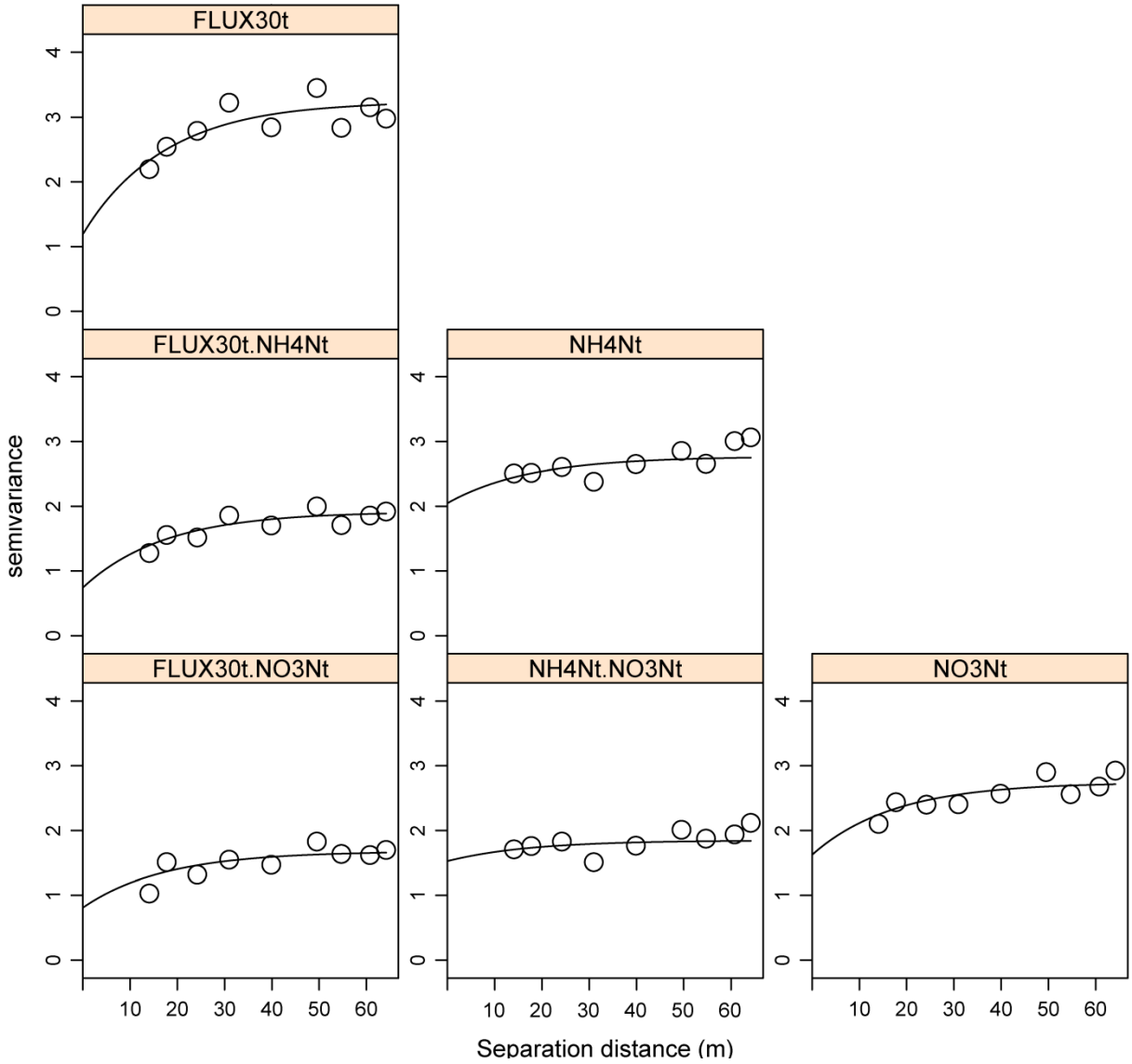

691

692 Figure 8

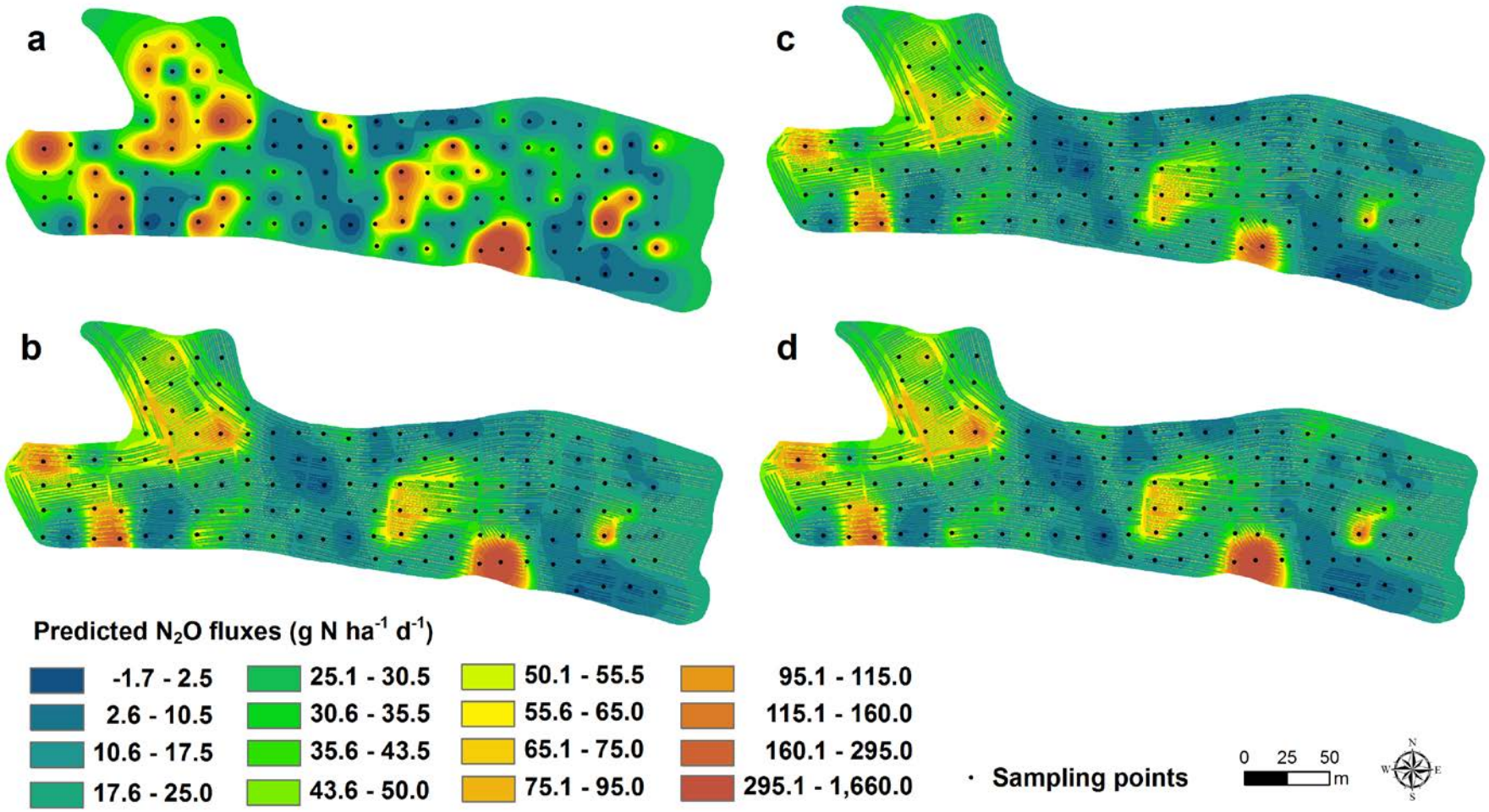

693

694 Figure 9

695

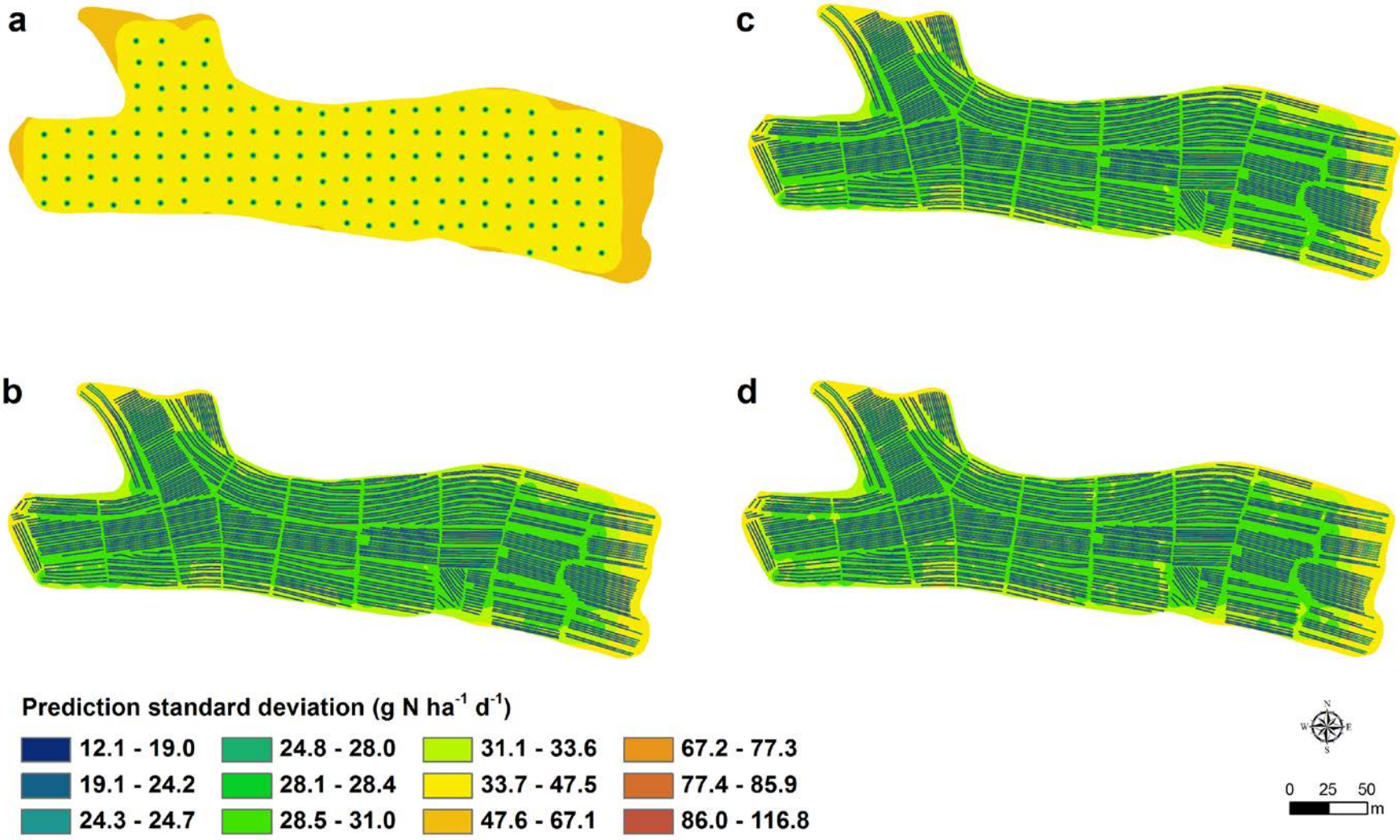
a
c
b
d
Prediction standard deviation (g N ha-1 d-1)
12.1 - 19.0
19.1 - 24.2
24.3 - 24.7
24.8 - 28.0
28.1 - 28.4
28.5 - 31.0
31.1 - 33.6
33.7 - 47.5
47.6 - 67.1
67.2 - 77.3
77.4 - 85.9
86.0 - 116.8
N
W
E
S
0 25 50
m

Figure 10